Astron. Astrophys. 321, 643–651 (1997)

ASTRONOMY
AND
ASTROPHYSICS

Some properties of sunspot umbral dots

A. Tritschler and W. Schmidt

Kiepenheuer-Institut für Sonnenphysik, Schöneckstr. 6, D-79104 Freiburg, Germany

Received 1 April 1996 / Accepted 16 October 1996

Abstract. High resolution Stokes-I spectra of the Zeeman-sensitive lines at λ 846.85 nm and λ 630.25 nm were used to determine the magnetic field strength and the brightness temperature of a simple, relatively symmetric sunspot umbra and its umbral dots (UDs).

We find a decrease in brightness temperature for central ($\sim$30 %) and peripheral UDs (20-25 %) compared to the surrounding quiet sun. This corresponds to a difference in temperature of about 1600 K and 1200-1400 K respectively.

The magnetic field strength within the umbra is derived from the Zeeman splitting of the Stokes-I profile. Field strengths within the umbra vary between 1500 and 3000 G. Further analysis of the λ 846.85 nm spectra indicates that the magnetic field strength within the umbral features is not significantly reduced neither for centrally ($\leq$ 3 %) nor for peripherically located UDs (1-2 %). The λ 630.25 nm line yields an enhanced weakening of field strength of 7 % for an isolated located UD.

The measured properties of UDs do not vary significantly during a 40 min observation sequence.

Key words: solar activity – sunspots – umbral dots

1. Introduction

The study of umbrae and the variety of their structural details play a key role in the unsolved issue of energy transport in sunspots. Umbral dots carry information on the magnetic structure and the thermal state of the near-surface layers of the umbra. They contribute up to 40 % to the umbral intensity at visible wavelengths (Adjabshirzadeh & Koutchmy 1983) and therefore represent a source of the observed umbral brightness. Reviews of the relevant observable parameters are given by García de la Rosa (1987) and Muller (1992).

Considering a model in which the sunspot consists of a single monolithic magnetic column, Knobloch & Weiss (1984) showed that in a nonlinear treatment of magnetoconvection vertical energy transport is occuring inside the rigid magnetic field structure. In their picture UDs are the visible consequence of coherent motions in convective cells with diameters of 250-300 km reaching down to a depth of $\sim$1500 km.

The so-called cluster model, proposed by Parker (1979) and elaborated by Choudhuri (1986), proceeds from the assumption that the sunspot magnetic field splits below the visible umbral photosphere in several individual bundles of flux tubes separated by nearly fieldfree solar plasma. Overstable convection can occur in these fieldfree regions and UDs are believed to be the manifestation for hot columns of gas, rising up between the magnetic ropes.

In a more recent theoretical study, Degenhardt & Lites (1993) investigate the behaviour of a thin vertical gas column embedded in a sunspot umbra using the thin flux tube approximation (Ferriz-Maz & Schüssler 1990).

The magnetic field strength in UDs should be greatly reduced at the visible surface and accompanied by substantial upflows ($\sim$ 10 km/s) if we believe the Parker/Choudhuri picture. The observable signatures in the model of Knobloch & Weiss would be large fluctuations in field strength due to the highly nonlinear oscillations, while Degenhardt & Lites predict only small velocity and magnetic field differencies in photospheric layers and an inverse field gradient in UDs.

However, these model characteristics are not in accord with existing observations. On the other hand observations of UDs are strongly influenced by the spatial resolution of the instrument and seeing conditions. Thus from the observational point of view it is as well difficult to rule out or confirm any of the models.

The brightness and temperature of UDs has been studied by various authors (e.g. Beckers & Schröter 1968; Koutchmy & Adjabshirzadeh 1981; Grossmann-Doerth et al. 1986; Sobotka et al. 1992a, 1992b; Ewell 1992; Sobotka et al. 1993) who agree that the wide range of measured UD contrasts and derived temperatures points to the existence of more than one kind of UDs, differing in their individual intrinsic development.

Spectroscopic investigations allow to infer the magnetic field strength inside umbrae. In observations of moderate spatial resolution ($\geq 1''$), UDs tend to show a slightly weaker field strength than the surrounding umbra. The claimed reduction in field strength varies between some 100 Gauss (Beckers & Schröter 1969; Adjabshirzadeh & Koutchmy 1983; Pahlke & Wiehr 1990) up to nearly 50 % (Kneer 1973).

Observations of higher spatial resolution show more contradicting results. Lites et al. (1991) find that UDs are not ac-

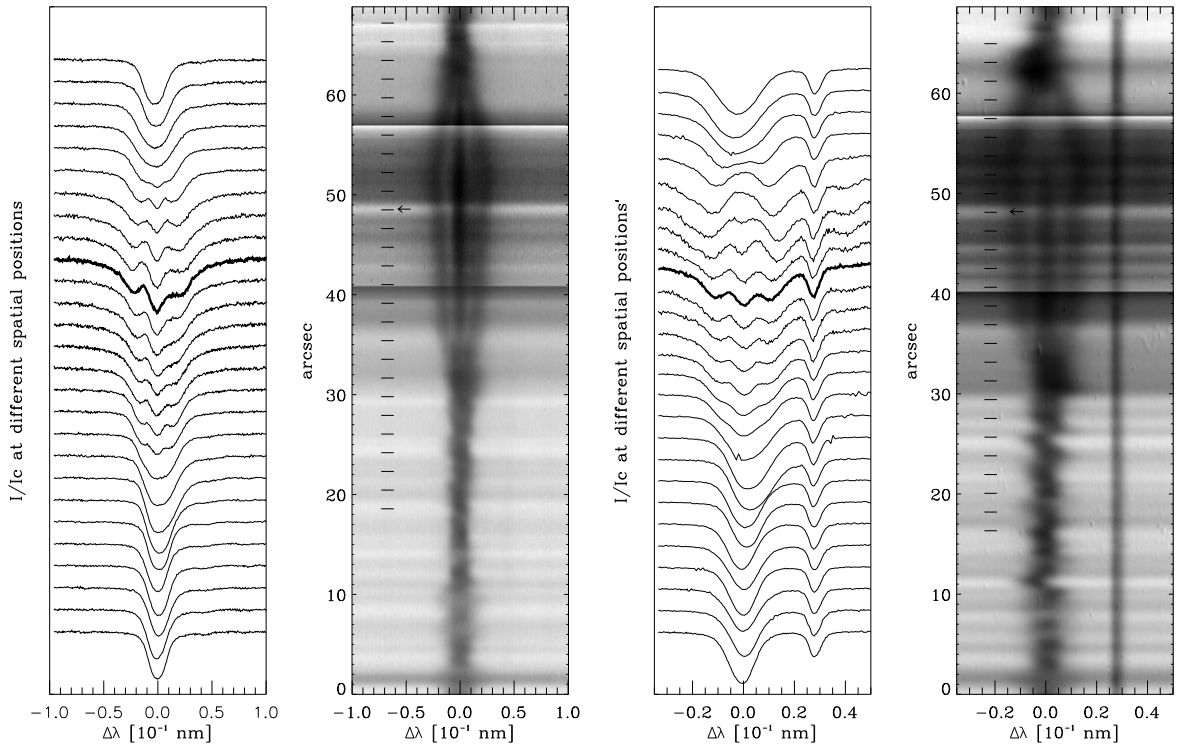

Fig. 1. Line profiles I/I_c along the slit and corresponding spectrogram. The lowermost profile was recorded at a position of 18.7 arcseconds in the corresponding spectrum, the following ones in steps of 1.87 arcseconds. Left: λ 846.85 nm, CUD1 sequence; right: λ 630.25 nm, CUD2 sequence. In both spectra the umbra is inserted in a different intensity scale. The position of the extracted line profiles is marked in the corresponding spectrogram. The thick lines are UD line profiles and their location in the spectrogram is marked with an arrow.

companied by significant variations of magnetic field strength at the visible surface. We refer to Grossmann-Doerth et al. (1986) and distinguish between central and peripheral UDs (CUDs and PUDs respectively). Schmidt & Balthasar (1994) find a field reduction in CUDs of ∼10-20 % and in PUDs of ∼5-10 %. In a more recent study Balthasar & Schmidt (1994) report about a decrease of magnetic field strength in bright umbral structures by 5-10 % for an infrared line. A weakening of the field strength of ∼20 % in PUDs and almost none in CUDs has been reported by Wiehr & Degenhardt (1993).

2. Observations

We analysed sunspot observations obtained during an observing run in 1991 with the 70 cm Vacuum Tower Telescope (VTT) located at the Observatorio del Teide, Izaña. A fairly regular medium sized sunspot (NOAA 6681) was selected with a diameter of about 40″ showing a considerable number of UDs in the slit-jaw pictures. Observations were made on June 19, when the spot was located at cos θ = 0.88.

The Echelle-Type spectrograph of the VTT was used to obtain spectrograms in two different spectral regions at λ 630.25 nm and λ 846.85 nm. A large format (1024×1024 pixel) CCD camera with a pixel size of 19 microns squared recorded the data set in 2×2 summing mode. With the image scale of the spectrograph in the focal plane of 4.″82 per mm the spatial FOV was 92″ with a pixel size of 0.″18. The spectral FOV is 0.2 nm due to the linear dispersion of the spectrograph of about 0.1 nm/cm in the red part of the visible spectrum. Raster scans of the sunspot were obtained by moving the solar image across the spectrograph. For the λ 630.25 nm (λ 846.85 nm) line the spot was scanned in 16 (14) steps of 0.5 arcseconds. The slit width was 80 μm corresponding to 0.″4 on the sun and the exposure time was 0.2 (0.4) seconds. With a step to step time of 5.4 seconds the repetition time for the rasters amounts to 86 (76) seconds.

The small size of UDs makes them difficult to track although the seeing conditions were quite good. Imperfect positioning of the slit during the exposure can cause a dot to disappear from the spectrogram. The data set we obtained consists of several time series taken first at λ 846.85 nm and then at λ 630.25 nm.

Fig. 1 shows two spectrograms of the observed wavelength regions and the spatial variation of the normalized intensity profiles on the left of them. The two scans do not represent the same cut, but they are from the same spot. On the blue side of the λ 630.25 nm line no data are available.

Since the spectra of the two lines were not recorded simultaneously, it was not possible to compare the umbral features in different wavelengths directly, thus no field gradient could be derived, neither in the UD nor in the inter-dot regions.

Table 1. Some relevant parameters of the observed lines.

Spectral line	Fe I λ 630.25 nm	Fe I λ 846.85 nm	Ti I λ 846.8 nm$^{(*)}$
Excitation potential	3.67 eV	2.21 eV	1.88 eV
Transition	$^5P_1$–$^5D_0$	$^5P_1$–$^5P_1$	$^3F_4$–$^3G_5$
Multiplet	816	60	150
Equivalent width	8.3 pm	12.8 pm	–
Landé factor	2.5	2.5	1.125
Exposure time	0.2 sec	0.4 sec	0.4 sec
Image scale (/pixel)	$0\farcs18\times0.40$ pm	$0\farcs18\times0.52$ pm	$0\farcs18\times0.52$ pm

$^{(*)}$ Exact wavelength is not known.

2.1. Line characteristics

The two Fe I lines are well suited for magnetic field measurements since both have an effective Landé factor of 2.5 and split into a simple Zeeman triplet. Unlike the λ 630.25 nm line the λ 846.85 nm line has an asymmetry in the σ-components, due to the presence of a Ti I blend whose wavelength and line strength are not exactly known (see Fig. 1). The σ_r-component is deformed, indicating that the blend is somewhat shifted to the red part relative to the Fe I line. Thus we cannot exclude that the blend may have an influence on the strength of the π-component seen in the λ 846.85 nm line. The Ti I line has a rather complicated splitting pattern with a $g_{\rm eff}$ of 1.125. The variation of the line profiles along the slit (see Fig. 1) indicates that the blend gets stronger with increasing magnetic field strength and with decreasing temperature.

Although the presence of the blend complicates the analysis of the λ 846.85 nm line, these observations represent independent measurements of the same sunspot region. We expect to gain information about higher photospheric layers than from the λ 630.25 nm line. The characteristics of the observed lines and some observational parameters are summarized in Table 1.

3. Data analysis

The first steps of analysis included flat fielding, dark current correction and the consideration of the effects of stray light. We took into account spectrally undispersed and dispersed scattered light. The former originates from e.g. the scattering of sunlight at randomly distributed dust particles inside the spectrograph which reaches the detector everywhere with the same intensity. The latter is related to light which is scattered into the umbra from outside the spot region.

We assume that the observed and the real intensity profile inside the umbra, $I_{\rm real}(\lambda)$ and $I_{\rm obs.}(\lambda)$ respectively, are related by

$$I_{\rm real}(\lambda) \;=\; I_{\rm obs.}(\lambda) \;-\; S_{\rm a}\, I_{\odot}(\lambda),$$

where $I_{\odot}(\lambda)$ denotes the intensity profile of the adjacent quiet sun and $S_{\rm a}\, I_{\odot}(\lambda)$ the contribution of atmospheric stray light to the umbral line profile. A similar relation can be formulated between the observed ($K_{\rm obs.}$) and the real ($K_{\rm real}$) continuum intensity ratio umbra/photosphere:

$$K_{\rm real} \;=\; K_{\rm obs.} \;-\; S_{\rm a}\;; \quad K_{\rm real} \;=\; \frac{I_{\rm real}}{I_{\odot}}\,, \quad K_{\rm obs.} \;=\; \frac{I_{\rm obs.}}{I_{\odot}}.$$

Assuming that $S_{\rm a}$ is more or less constant inside the umbra, the knowledge of either the real umbral intensity contrast $K_{\rm real}$ or the amount of stray light $S_{\rm a}$ enables to reconstruct the real umbral intensity profiles.

Owing to the lack of additional data (e.g. aureoles) that could enable us to determine the actual amount of stray light, we adopted a literature value (Maltby et al. 1986) for the umbral continuum contrast $K_{\rm real}$ of 0.21 at λ 846.85 nm.

In the next step we selected scans that show well defined UDs: two series of the λ 846.85 nm line, each consisting of 27 spectra taken between 8:44 and 9:23 UT and one series of the λ 630.25 nm line consisting of 25 spectra recorded between 11:06 and 11:40 UT. There are various UDs scattered over the umbra observed. The isolated UDs in one of the λ 846.85 nm sequences (CUD1) and in the λ 630.25 nm sequence (CUD2) are located well within the umbra. The UD pair in the second λ 846.85 nm sequence is found close to the umbra-penumbra boundary (PUDs), where the intensity gradient is large and the magnetic field lines are much more inclined against the surface normal than in the central part of the umbra. In the following PUD1 denotes the UD closer to the penumbra and PUD2 the UD closer to the central part of the umbra. Besides this, the slices belonging to the single dot series pass through the darkest parts of the umbra, whereas those of the double dot series cut through the periphery of the umbra.

3.1. Magnetic field strength and brightness temperature

Spectroscopic determinations of solar magnetic field strength make use of the Zeeman effect. For the simple case of a triplet the equation

$$\Delta\lambda_{\rm B} \;=\; 4.67\times10^{-12}\, g_{\rm eff}\, \lambda_0^2\, |\mathbf{B}|,$$

specifies the relationship between the wavelength shift of the σ-components $\Delta\lambda_{\rm B}$ relative to the wavelength of the unshifted line position λ_0 given in nm and the magnetic field strength $|\mathbf{B}|$ in Gauss. Hence the Zeeman equation can be used to infer the field

strength from the observed broadening of the Stokes-I profile if the line is sufficiently split. This direct method is limited to the case, where the line-forming layer is permeated by a strong magnetic field and the inclination to the line-of-sight is small (Balthasar & Schmidt 1993).

Since the blend of the λ 846.85 nm line deforms the σ_r-component and may also affect the position of the π-component the direct method seems not to be appropriate to determine the field strength. In order to obtain more reliable results, we calculated synthetic line profiles and fitted them to the observed ones (see Sect. 4).

The brightness temperature T was derived by converting the continuum intensity I into temperature via the Planck law and assuming local thermal equilibrium :

$$T = \frac{hc}{\lambda k} \left[\ln \left(1 + \frac{I_\odot}{I} \left\{ \exp \left(\frac{hc}{\lambda k T_\odot} \right) - 1 \right\} \right) \right]^{-1}$$

where $I_\odot$ and $T_\odot$ is the quiet sun continuum intensity and temperature respectively.

3.2. Determination of the local background

We considered the UD brightness under the following aspect (Koutchmy & Adjabshirzadeh 1981): the central intensity of the UD profile $I_{\rm dot}$ is measured above a local pseudo-background level $I_{\rm bg}$ obtained by interpolating between two footpoints as seen from each side of the UD. A similar interpolation method was used to derive the ratio of magnetic field strength inside the UD to that of the surrounding dark umbral material. The knowledge of the variation of the field strength inside the umbra enables to attribute a field strength value to the footpoints. Between these values we interpolate linearly on the local magnetic background. The magnetic profile between the two footpoints is approximated through a second order polynomial fit. Together with the position of the UD in the spectra a value of magnetic field strength can be attached to the UD and the umbral pseudo-background (see Fig. 2). This technique works out well for an isolated UD located centrally in the umbra. For the case of two adjacent UDs - as in sequence PUD1/2 - a slightly different method was used. Since the two PUDs are magnetically unresolved, the interpolation on the local magnetic background was done only between the outer footpoints.

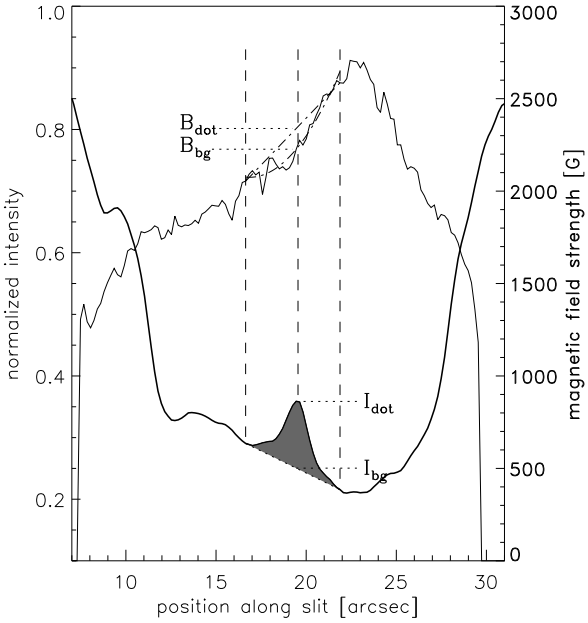

Fig. 2. Determination of the local intensity and magnetic background. Shown are the variation of the magnetic field strength (thin line) and the intensity (thick line) along the slit. Magnetic field values below 1000 G are not reliable.

4. Line profile calculations

We calculated synthetic line profiles and fitted them to observed line profiles in order to derive the magnetic field strength. Therefore we used a Stokes diagnostic code described by Grossmann-Doerth et al. (1988) and Grossmann-Doerth (1993). This version employs the DELO-method for solving the Unno-Rachovsky equations (Rees et al. 1989) numerically and provides the line depression contribution functions necessary to infer the formation height of the absorption line under consideration. The computations were all done with plane parallel models of either the quiet or the active (e.g. umbra, penumbra) solar atmosphere. We used the photospheric model T93 of Schleicher (1976), the penumbra model of Ding & Fang (1989), the umbral model M4 of Kollatschny et al. (1980) and in addition two umbral models IAC-C and IAC-H corresponding to "cool" and "hot" spots (Collados et al. 1994).

Following the matrix technique described by Balthasar & Schmidt (1993), we computed synthetic line profiles for field values from 0 to 3100 G with 50 G increments and for angles between 0 and 90 degrees with 10 degree steps. In all calculations we applied a field gradient of 2 G/km (Pahlke & Wiehr 1990). This results in a matrix of line profiles, whose entries are compared with the observed profiles.

4.1. Oscillator strengths

Unlike to the λ 630.25 nm line, where all relevant atomic parameters, in particular the value for the combined oscillator strength and abundance $gf\epsilon$ and the *Van-der-Waals* fudge factor are well known, we have less information of those parameters for the λ 846.85 nm line and the Ti I blend.

In a first approach the value for the weighted oscillator strength of the neutral titanium line given by Vakulenko & Savanov (1990) was adopted. We assumed the solar Ti abundance to be at logϵ=5.08 (Blackwell et al. 1987). For the Fe content in the solar atmosphere a value of logϵ=7.50 was adopted (Ross & Aller 1976). The Van-der-Waals fudge factors for both lines at λ 846.85 nm were set to a value of 2 because the excitation energy is rather low. Since we have no clue for the corresponding log$gf\epsilon$ value of the Fe I λ 846.85 nm line, we compared synthetic line profiles calculated with different loggf with those of the Kitt-Peak spectral atlas using the model T93. In order to

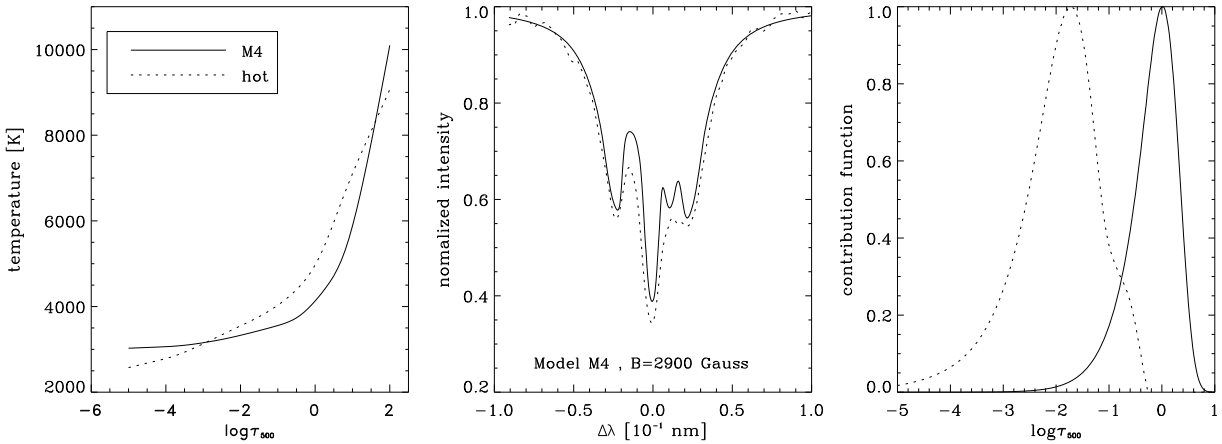

Fig. 3. Left: the temperature stratifications of the used umbral models M4 (Kollatschny et al. 1980) and IAC-H (Collados et al. 1994) as function of optical depth (continuum, 500 nm). Middle: an umbral line profile of the λ 846.85 nm line (dotted) and the synthetic line profile calculated with the M4 model (solid). Right: the line depression contribution function of the line core (dotted) and the contribution function of the emergent continuum intensity (solid) of the λ 846.85 nm line as function of optical depth. Both CFs are calculated with the model M4.

Table 2. Atomic parameters of the lines at λ 846.85 nm .

Element	logϵ	log$gf_{\rm Lit.}$	loggf	log$gf\epsilon$
Fe I	7.50	–	-2.24	-6.74
Ti I	5.08	-1.51	-1.17	-8.09

compensate for unresolved velocity fields the synthetic profiles at λ 846.85 nm have been convolved with a Gaussian corresponding to 2.0 km/s. A further convolution with a Gaussian of 0.7 pm was applied in order to match the effective spectral resolution of the spectrograph. This comparison yields a value loggf=-2.24 for the iron line at λ 846.85 nm. Applying the obtained values to calculations with the umbral model M4 shows that the synthetic profiles fit the observed ones rather badly. A further variation of the loggf values for both lines was therefore performed until finally an acceptable agreement between observed and synthetic line profiles was found for both the quiet sun and for the umbra. The atomic parameters are listed in Table 2.

4.2. Formation height of the lines

The determination of height levels in UDs is a difficult task, limited by the lack of information about the actual temperature and pressure stratification for the different umbral regions. In order to overcome this, the observed umbral and UD line profiles are compared with the computed synthetic profiles from the different model atmospheres. We regarded those model atmospheres for further use which reproduce best the observed profiles and give the right continuum intensity ratio of umbra to photosphere. These were used to derive the height levels of the continuum and the line core. M4 reflects best the situation inside the darkest part of the umbra while the profiles of the quiet sun are best reproduced by the model T93. Fig. 3 (middle) shows an umbral line profile taken from the darkest part of the umbra (dashed) and the corresponding synthetic profile (solid). The direct measurement yields 2700 G, whereas the comparison with synthetic line profiles gives an actual field strength of about 2900 G.

Table 3. Height levels of the observed lines inside the umbra and outside the spot. Calculations for the quiet sun and the umbra were done with the model T93 and M4 respectively; h_0 – continuum, $h_{\rm c}$ – line core.

λ [nm]	quiet sun		umbra	
	h_0 [km]	$h_{\rm c}$ [km]	h_0 [km]	$h_{\rm c}$ [km]
Fe 846.85	20	420	30	200
Fe 630.25	10	370	15	180

Contribution functions (CF) were used to extract the information about the line-forming layers. The weighted center h of the CF is determined for the continuum (h_0) and the line core ($h_{\rm c}$). All calculations concerning the continuum are done with the CFs for the emergent intensity, while for the line core the CFs for the line depression have been used. Two typical CFs are displayed in Fig. 3 (right). The relationship between the optical depth τ and the geometrical height h is given by the model atmospheres.

Table 3 summarizes the results derived from line profiles representative for the quiet sun and the umbra. In the umbra as well in the unperturbed photosphere the continuum of both lines forms near the level where the continuum optical depth $\tau_{\rm c}$ (for a wavelength of 500 nm) equals unity, whereas the line core at least outside the spot is formed in high layers. Single line calculations for the λ 846.85 nm line indicate that this is mainly due to the neutral iron line.

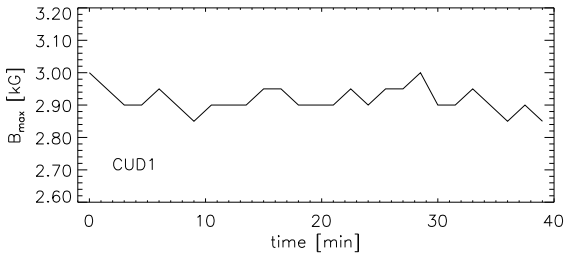

Fig. 4. The maximum value of magnetic field strength $B_{\rm max}$ of the CUD1 sequence as a function of time. The magnetic field strength is derived from a comparison with synthetic line profiles.

Table 4. Formation heights of the UDs, derived from the IAC-H model; h_0 – continuum, $h_{\rm c}$ – line core.

λ [nm]		umbral dot	
		h_0 [km]	$h_{\rm c}$ [km]
Fe 846.85	PUD1/2	30	180
	CUD1	30	170
Fe 630.25	CUD2	20	130

The comparison with the other model atmospheres reveals that the IAC-H model of Collados et al. (1994) matches best the UD line profiles. The temperature stratifications used for the calculations of the synthetic line profiles are displayed in Fig. 3 (left). The resulting formation heights are listed in Table 4. Both, the emergent contiuum intensity and the line depression of the CUD2 (λ 630.25 nm) originate from deeper layers than those from the PUDs and the CUD1 (λ 846.85 nm). A direct comparison of geometric height scales in and outside umbral dots is not possible. This could be only done knowing the Wilson depression of the different umbral regions.

5. Results and discussion

5.1. Weakening of the magnetic field in UDs

The variation of magnetic field strength inside the umbra shows the well known inverse correlation with the variation of intensity. Fig. 4 shows the temporal variation of the maximum magnetic field strength in each sequence obtained with the Stokes synthesis code. The variation of the umbral field strength with time is subject to fluctuations, with no significant variation over the whole observing run. The influence of the titanium blend on the position of the π-component seen in the λ 846.85 nm line may lead to a misjudgement of the magnetic field strength but this is a second order effect, which affects the determination of the magnetic field ratios by a small amount.

Fig. 5 displays the ratios of $B_{\rm dot}/B_{\rm bg}$ versus time for the selected sequences. The derived values for $B_{\rm dot}/B_{\rm bg}$ from the synthetic line profiles are slightly lower than 1.0 and the average field reduction amounts to $\sim$ 3 % for the CUD1 sequence and 1-2 % for the PUD1/PUD2 sequence. The weakening of magnetic field strength is higher in the CUD2 sequence and amounts to $\sim$ 7 %. In Fig. 5 are also plotted the field strength ratios of UD to adjacent umbra $B_{\rm dot}/B_{\rm out}$ and $B_{\rm dot}/B_{\rm in}$, where $B_{\rm out}$ and $B_{\rm in}$ denote the field strengths as seen to each side of the UD, either in direction to the penumbra (outer footpoint) or to the deep umbra (inner footpoint). These ratios show a significant deviation from unity. This can be explained by the overall variation of the umbral magnetic field strength and the fact, that $B_{\rm out}$ and $B_{\rm in}$ are measured at a position considerably beside the UD, whereas $B_{\rm bg}$ approximates the umbral field strength that would be present at the UD position, if there would not be an UD.

Further systematic errors are introduced due to the different temperature of UDs compared to the surrounding umbra. Thus the iso-τ-levels belong to different heights in- and outside UDs. Therefore we compare field strengths in UDs with those of the adjacent umbra, although these measurements correspond to different geometrical heights inside the umbral atmosphere. As mentioned before, our results concerning the height levels of the observed lines in and outside UDs cannot be used for a direct comparison of geometric height scales, since they originate from different model atmospheres and we do not know the difference in height between the $\tau_{\rm c}$ = 1 levels of the umbral models M4 and IAC-H. In order to overcome this lack of information we use the theoretical model of Degenhardt & Lites (1993). They find that the continuum level of the UD is shifted towards higher layers compared to the surrounding umbra (see Fig. 2a, page 387). The difference in height between the $\tau_{\rm c}$ = 1 level in- and ouside the UD amounts roughly to 100 km for a typical model. Adding this value to the results in Table 3 shows that the observed spectral lines originate higher in the UDs than in the surrounding umbra. If we further adopt an umbral field gradient of 2 G/km, the shift of 100 km results in a decrease of the background magnetic field strength $B_{\rm bg}$. Hence we underestimate the ratio $B_{\rm dot}/B_{\rm bg}$ by a few percent. For equal geometrical heights the reduction of magnetic field strength in UDs becomes negligible even for the λ 630.25 nm line.

5.2. Temperatures and intensity contrasts of UDs

We investigated the brightness temperature and intensity contrast of the observed UDs. Fig. 6 (left panel) displays the temporal variation of the calculated temperature ratios $T_{\rm dot}/T_{\rm bg}$ and $T_{\rm dot}/T_{\odot}$. The right panel shows the variation of the UD-to-background intensity ratio $I_{\rm dot}/I_{\rm bg}$ as a function of time for the continuum and the line core. The intensity contrasts indicate that the PUD1 vanishes after 33 min, while the PUD2 and the CUD1 slowly fade away during the observation interval. No such trend is visible in the CUD2 sequence. Seeing shows fluctuations but does not become bad towards the end of the sequences, so that the observed fading of the UDs is real.

Table 5 includes all results of the analysis as time averages for the selected sequences. Since the measured intensities are subject to fluctuations caused by different effects, some care must be taken by calculating averages. All measurements indicating either bad seeing, an imperfect positioning of the slit,

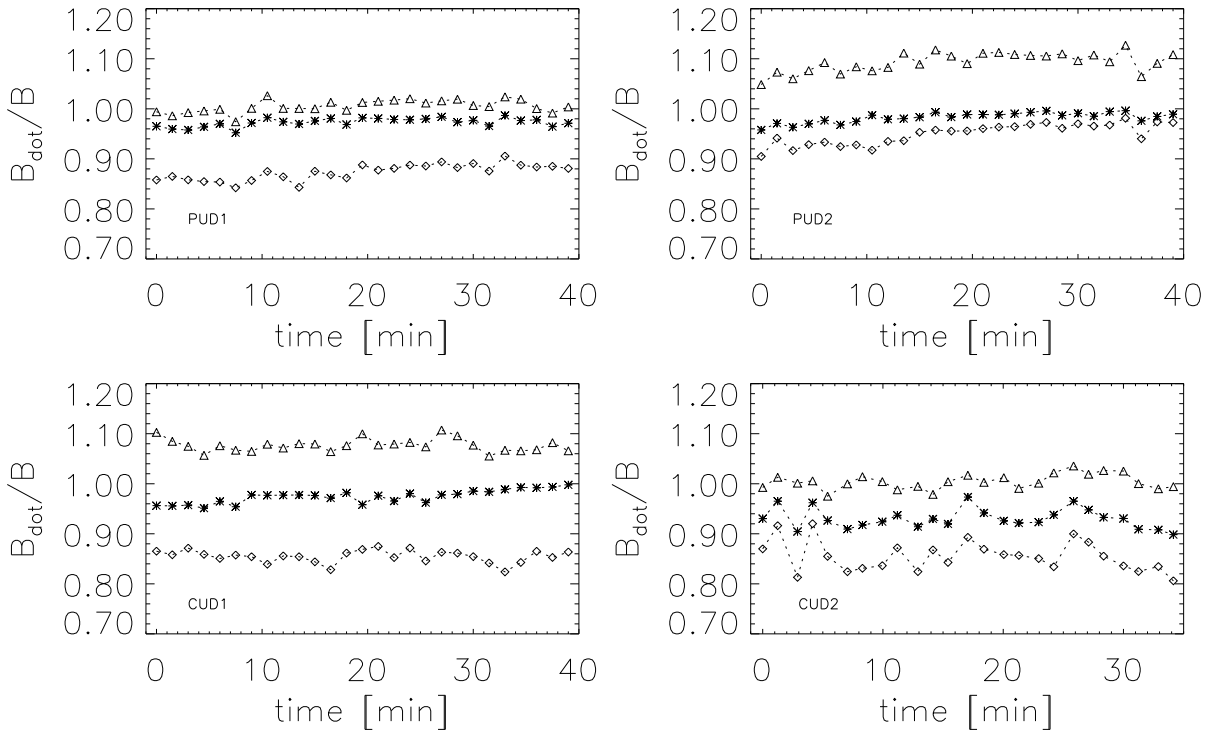

Fig. 5. Magnetic field reduction in UDs. The magnetic field ratios $B_{\rm dot}/B_{\rm bg}$ ($*$), $B_{\rm dot}/B_{\rm in}$ ($\diamond$) and $B_{\rm dot}/B_{\rm out}$ ($\triangle$) versus time are shown for the selected sequences of the λ 846.85 nm line and the λ 630.25 nm line. bg – umbral background, in – UD footpoint towards umbra, out – UD footpoint towards penumbra.

Table 5. Results of the UD analysis at λ 846.85 nm and λ 630.25 nm.
$\Delta T_\odot$ – Temperature difference UD-quiet sun. $\Delta T_{\rm bg}$ – Temperature difference UD-background. $(\frac{B_{\rm dot}}{B_{\rm bg}})_{\rm cal.}$ – magnetic field strength ratio UD-to-background derived from the synthetic line profiles. The indices 0 and c refer to continuum and line core respectively.

Sequence	$\frac{T_{\rm dot}}{T_\odot}$	$\frac{T_{\rm dot}}{T_{\rm bg}}$	$\Delta T_\odot$	$\Delta T_{\rm bg}$	$(\frac{I_{\rm dot}}{I_\odot})_0$	$(\frac{I_{\rm dot}}{I_{\rm bg}})_0$	$(\frac{I_{\rm dot}}{I_\odot})_{\rm c}$	$(\frac{I_{\rm dot}}{I_{\rm bg}})_{\rm c}$	$(\frac{B_{\rm dot}}{B_{\rm bg}})_{\rm cal.}$
PUD1	0.80	1.06	1160	270	0.47	1.26	0.40	1.19	0.98
PUD2	0.75	1.05	1440	190	0.37	1.19	0.29	1.15	0.99
CUD1	0.73	1.06	1560	240	0.33	1.27	0.24	1.19	0.97
CUD2	0.72	1.08	1630	300	0.21	1.52	0.23	1.39	0.93

or the possible disappearence of the UD due to the intrinsic development, have been excluded.

The average values of the temperature reduction $T_{\rm dot}/T_\odot$, the temperature difference Quiet Sun - UD, $\Delta T_\odot$, and the continuum intensity contrast $(I_{\rm dot}/I_\odot)_0$ show a dependence of the radial position of the UD inside the umbra (see Table 4). This effect can partially be due to an insufficient stray light correction (see Sect.3) concerning the PUD1/2 sequence.

The simplified stray light procedure neglects the spatial variation of the stray light across the spot and leads to a certain undercorrection near the umbra-penumbra boundary and hence to an overestimation of intensities $I_{\rm dot}$ and temperatures $T_{\rm dot}$ for the peripheral UDs. This is in turn partially compensated by using photospheric brightness instead of penumbral intensity. On the other hand, a stronger correction for stray light would lead to higher continuum contrasts $(I_{\rm dot}/I_{\rm bg})_0$, together with a decrease of the temperature reduction $T_{\rm dot}/T_\odot$ and an increase of the temperature difference $\Delta T_\odot$. Thus the PUDs would become much brighter but also much more inconspicuous than the CUDs concerning their temperature signatures. Thus the observed difference between CUDs and PUDs cannot be explained by an insufficient stray light correction. We therefore conclude that the radial dependence is real and there exists a physical difference between CUDs and PUDs.

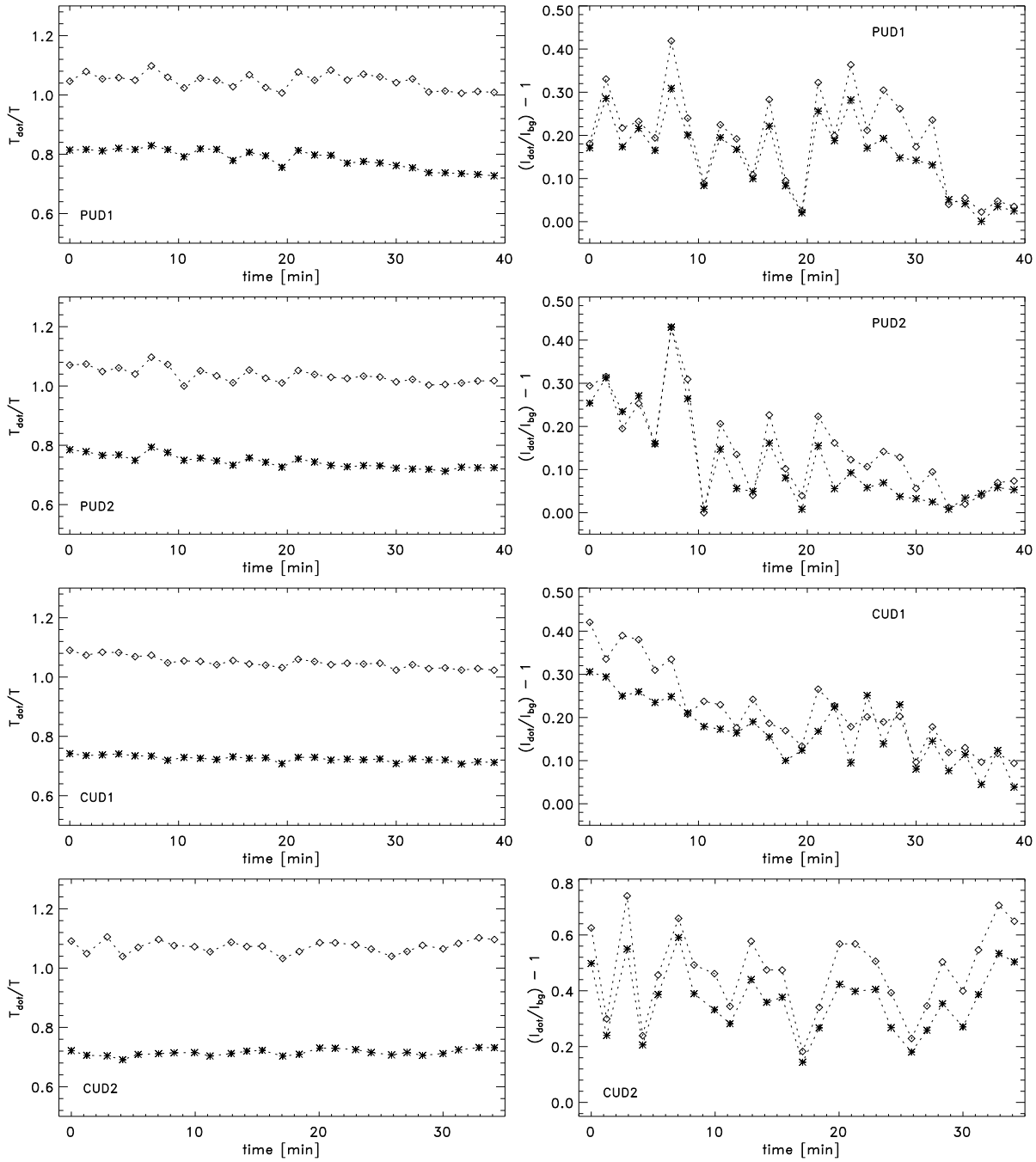

Fig. 6. Brightness temperature and intensity contrast of UDs. Shown are the UD brightness temperatures relative to the quiet sun $T_{\rm dot}/T_{\odot}$ ($*$) and the umbral background $T_{\rm dot}/T_{\rm bg}$ ($\diamond$) versus time (left panel) and the UD contrasts measured in the continuum ($*$) and the line core ($\diamond$) (right panel).

6. Conclusions

We have empirically determined brightness temperatures and magnetic field strengths of small-scale umbral features. The results of our observations can be summarized as follows:

(a) From the absence of a significant reduction of field strength in the UDs ($\leq$3 %) we concluded that UDs are "magnetically invisible" in the regions where the Fe I λ 864.8 nm line is formed.

(b) We find a decrease of brightness temperature in UDs by $\sim$30 % for CUDs and by 20-25 % for PUDs compared to the surrounding quiet photosphere

(c) Umbral dots show an excess of brightness temperature by $\sim$300 K relative to the umbral background.

(d) The UDs are still visible in the height of the line core, but with reduced intensity contrast.
(e) The observed UDs gradually fade away during the 40 min time interval of our measurements.

Our derived continuum contrasts are in agreement with other observations (Koutchmy & Adjabshirzadeh 1981; Lites et al. 1991; Sobotka et al. 1992a, 1992b; Sobotka et al. 1993). The investigated UDs show brightness temperatures of more than 1000 K below those of the photosphere. Grossmann-Doerth et al. (1986) find a temperature decrease of up to 1000 K in UDs. In contrast, results from two-colour analysis (Beckers & Schröter 1969, Koutchmy & Adjabshirzadeh 1981) or inhomogeneous modelling of sunspot umbrae (Koutchmy & Adjabshirzadeh 1981; Pahlke & Wiehr 1990) indicate photospheric or nearly photospheric temperatures of UDs.

The Fe I λ 864.8 nm line used in this work forms somewhat higher in the solar atmosphere compared to the Fe I λ 630.25 nm line and other lines used for spectroscopic investigations of UDs. Although other recent investigations of UDs yield higher magnetic field reductions (Balthasar & Schmidt 1993; Wiehr & Degenhardt 1993; Balthasar & Schmidt 1994), our results are in qualitative agreement with these observations, if they are seen as a consequence of different formation heights of the spectral lines inside and outside the umbral features and the height dependence of the magnetic field.

Our findings support the idea that UDs are phenomena of the deep umbra (Degenhardt & Lites 1993). They are best visible only at the continuum level of the umbral photosphere and are rather inconspicuous in the regions of line formation, where all measurements of magnetic field strength and material motions are made.

Acknowledgements. We like to thank Drs. Uli Grossmann-Doerth, Horst Balthasar and Michael Knölker for their helpful comments on the manuscript and are very much indebted to Prof. Dr. W. Mattig for his support of this investigation. We also like to thank the referee for critical reading of the manuscript and for valuable suggestions that helped to improve the paper.

References

Adjabshirzadeh, A., Koutchmy, S. 1983, A&A, 122, 1
Balthasar, H., Schmidt, W. 1993, A&A, 279, 243
Balthasar, H., Schmidt, W. 1994, A&A, 290, 649
Beckers, J.M., Schröter, E.H. 1968, Solar Phys., 4, 303
Beckers, J.M., Schröter, E.H. 1969, Solar Phys., 10, 384
Blackwell, D.E., Booth, A.J., Menon, S.R.L., Petford, A.D. 1987, A&A, 180, 229
Choudhuri, A.R. 1986, ApJ, 302, 809
Collados, M., Martínez Pillet, V., Ruiz Cobo, B., del Toro Iniesta, J.C., Vázquez, M. 1994, A&A, 270, 494
Degenhardt, D., Lites, B.W. 1993, ApJ, 404, 383
Ding, M.D., Fang, C. 1989, A&A, 225, 204
Ewell, M.W. 1992, Solar Phys., 137, 215
Ferriz Maz, A., Schüssler, M. 1990, Geophysical Monograph, 58, 141
García de la Rosa, J.I. 1987, in The Rôle of Fine-Scale Magnetic Fields on the Structure of the Solar Atmosphere, E. Schröter, M. Vázquez, A. Wyller (eds.), Cambridge University Press, 140
Grossmann-Doerth, U. 1993, A&A, 285, 1012
Grossmann-Doerth, U., Schmidt, W., Schröter, E.H. 1986, A&A, 156, 347
Grossmann-Doerth, U., Larsson, B., Solanki, S.K. 1988, A&A, 204, 266
Kneer, F. 1973, Solar Phys., 28, 361
Knobloch, E., Weiss, N.O. 1984, MNRAS, 207, 203
Kollatschny, W., Stellmacher, G., Wiehr, E., Falipou, M.A. 1980, A&A, 86, 245
Koutchmy, S., Adjabshirzadeh, A. 1981, A&A, 99, 111
Lites, B.W., Bida, T.A., Johannesson, A., Scharmer, G.B. 1991, ApJ, 373, 683
Maltby, P., Avrett, E.H., Carlsson, M. et al. 1986, ApJ, 306, 284
Muller, R. 1992, in Sunspots: Theory and Observations, J.H. Thomas and N.O. Weiss (eds.), Dordrecht Kluwer, 175
Pahlke, K.-D., Wiehr, E. 1990, A&A, 228, 246
Parker, E.N. 1979, ApJ, 234, 333
Rees, D.E., Murphy, G.A., Durrant, C.J. 1989, ApJ, 339, 1093
Ross, J.E., Aller, L.H. 1976, Sci, 191, 1223
Schleicher, H. 1976, Thesis, Göttingen
Schmidt, W., Balthasar, H. 1994, A&A, 283, 241
Sobotka, M., Bonet, J.A., Vázquez, M. 1992a, A&A, 257, 757
Sobotka, M., Bonet, J.A., Vázquez, M. 1992b, A&A, 260, 437
Sobotka, M., Bonet, J.A., Vázquez, M. 1993, ApJ, 415, 832
Vakulenko, D.A., Savanov, I.S. 1990, I. Krym. Astr. Obs., 82, 87
Wiehr, E., Degenhardt, D. 1993, A&A, 278, 584

This article was processed by the author using Springer-Verlag LaTeX A&A style file *L-AA* version 3.